

# Magnetic $H$ - $T$ phase diagram of holmium orthoferrite for $H \parallel b$

G. P. Vorob'ev, A. M. Kadomtseva, I. B. Krynetskiĭ, and A. A. Mukhin

Moscow State University

(Submitted 28 May 1990; resubmitted 29 June 1990)

Zh. Eksp. Teor. Fiz. **98**, 1726-1736 (November 1990)

Phase transitions in a magnetic field  $H \parallel b$  ( $H \leq 60$  kOe) have been studied for the first time on the basis of a comprehensive investigation of the magnetic and magnetoelastic properties of  $\text{HoFeO}_3$  and a corresponding theoretical analysis; the experimental and theoretical  $H$ - $T$  phase diagrams agree completely. The rich topology of the phase diagrams is manifest in the existence of various spin reorientational (SR) phase transitions ( $\Gamma_{23} \rightarrow \Gamma_{34}$ ,  $\Gamma_{23} \rightarrow \Gamma_{1234}$ ,  $\Gamma_{1234} \rightarrow \Gamma_{34}$ ), due to the appearance of an instability in the magnetic structure as the lower energy levels of  $\text{Ho}^{3+}$  ions approach one another (a magnetic analog of the Jahn-Teller effect), and also the existence of isostructural SR transitions between two spatial angular phases. It is shown theoretically that the topology of the high-field part of the  $H$ - $T$  phase diagram (for  $H > 50$ - $60$  kOe) depends strongly on the magnitude and sign of the isotropic R-Fe exchange constant, which usually does not play a significant role in the magnetic properties of orthoferrites. An unusual SR transition ( $H \geq 100$  kOe) is predicted, at which the spins of  $\text{Fe}^{3+}$  ions reorient with increase in field from a perpendicular state to a state parallel to the external field ( $\Gamma_{34} \rightarrow \Gamma_{13}$ ) (inverse spin-flop transition); in higher fields the usual spin-flop transition ( $\Gamma_{13} \rightarrow \Gamma_{34}$ ) takes place.

## 1. INTRODUCTION

Although a large amount of work<sup>1-3</sup> has been devoted to the study of the magnetic properties of holmium orthoferrite, a number of fundamental features of its magnetic behavior have hardly been studied. For example, up until now the phase diagrams for  $H \parallel b$  have not been investigated experimentally for the most interesting orientational transition produced by the onset of instability on the crossing (approach) in a field of the lowest energy levels of the  $\text{Ho}^{3+}$  ions in non-equivalent positions (the magnetic analog of the Jahn-Teller effect).<sup>4,5</sup> New basic properties in the form of the  $H$ - $T$  phase diagram of  $\text{HoFeO}_3$  for  $H \parallel b$  can arise because of an appreciable contribution to the anisotropy energy in the  $ab$  plane, determined by the Van Vleck mechanism, associated with admixture of excited states of the  $\text{Ho}^{3+}$  ion to its ground state, and stabilizing the antiferromagnetic structure  $\Gamma_1 (G_y)$ . To this contribution is due the unusual spontaneous orientational transitions in  $\text{HoFeO}_3$  accompanying the emergence of the spins from the  $ac$  plane to the  $bc$  plane:  $\Gamma_4 \rightarrow \Gamma_{24} \rightarrow \Gamma_{12} \rightarrow \Gamma_2$  ( $G_x \rightarrow G_x G_z \rightarrow G_z G_y \rightarrow G_z$ , where  $G$  is the antiferromagnetism vector and  $x, y, z$  correspond to the rhombic axes  $a, b, c$  of the crystal). The existence of such a Van Vleck contribution to the anisotropy energy of  $\text{HoFeO}_3$  can lead, for phase transformations in a field  $H \parallel b$ , to reorientation of the antiferromagnetism vector  $G$  from the  $c$  axis ( $\Gamma_2 (G_z)$ ) either to the  $a$  axis [ $\Gamma_4 (G_x)$ ] or to the  $b$  axis [ $\Gamma_1 (G_y)$ ], i.e. to a state with  $G \parallel H \parallel b$ . In the latter case, evidently, further phase transitions (spin-flop) are possible.

We have undertaken studies of the magnetic and magnetoelastic properties of a  $\text{HoFeO}_3$  single crystal for  $H \parallel b$  with the aim of establishing the character and sequence of the orientational transitions which then arise, and to construct the corresponding  $H$ - $T$  phase diagram.

## 2. EXPERIMENTAL RESULTS

Measurements of the magnetization, thermal expansion and magnetostriction were carried out on  $\text{HoFeO}_3$  single crystals grown by the method of spontaneous crystallization from a solution in a melt of lead compounds.

Figure 1 shows magnetization curves measured along the  $b$  axis of the rhombic crystal in the low-temperature region. It can be seen that for a certain value of the field, discontinuities are observed on the magnetization curves, and shift to higher fields as the temperature is raised, then becoming less sharp. In order to determine whether the observed anomalies in magnetization are associated with spin reorientation, a measurement was also made of the field dependence of magnetostriction, since this is a characteristic sensitive to a change in the magnetic structure of a crystal, arising on spin reorientation. Magnetostriction isotherms are shown in Fig. 2, measured along the  $a, b, c$  crystal axes on applying a magnetic field  $H \parallel b$ . Sharp changes in magnetostriction characteristic of spin reorientation (SR) transitions appear on the field dependences of magnetostriction at just those fields at which discontinuities of magnetization are observed. In the low temperature region magnetostriction for some value of the field changed practically discontinuously, while on increasing the temperature the orienta-

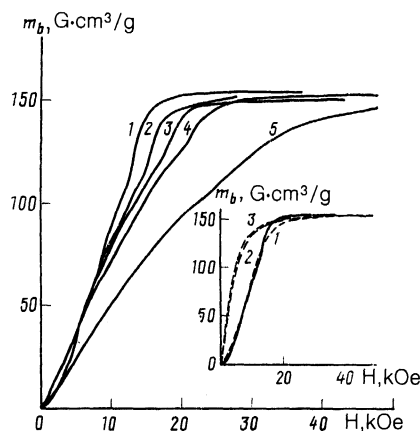


FIG. 1. Magnetization curves of a  $\text{HoFeO}_3$  crystal along the  $b$  axis; 1)  $T = 1.85$  K; 2) 2.95 K; 3) 4.2 K; 4) 5.9 K; 5) 11.5 K. The inset shows the magnetization curves of  $\text{HoFeO}_3$  at  $T = 1.85$  K. The full line is experiment, the dashed lines 1, 2, 3 are theoretical magnetization curves in the phases  $\Gamma_{23}$ ,  $\Gamma_{13}$  and  $\Gamma_{34}$  respectively.

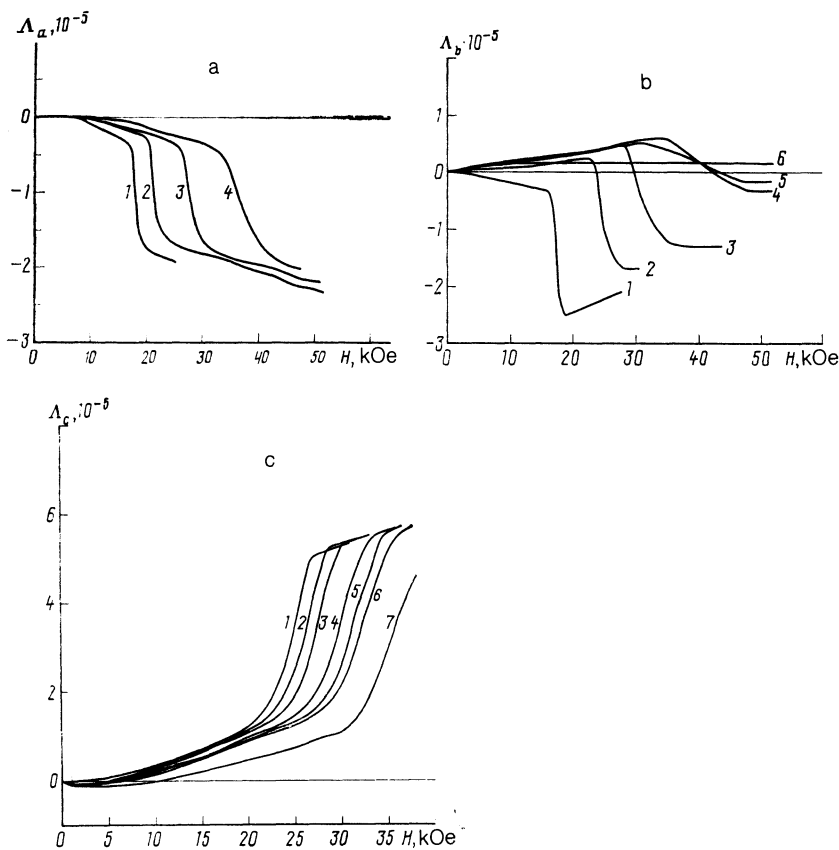


FIG. 2. Magnetostriction isotherms of  $\text{HoFeO}_3$  for  $\mathbf{H} \parallel \mathbf{h}$  along the crystal axes (a)  $a$ , (b)  $b$  and (c)  $c$ : a) 1— $T = 3.7$  K; 2— $4.9$  K; 3— $7.3$  K; 4— $14.2$  K; b) 1— $T = 4.2$  K; 2— $7.8$  K; 3— $12.9$  K; 4— $28.4$  K; 5— $34.7$  K; 6— $54$  K; c) 1— $T = 4.2$  K; 2— $5.1$  K; 3— $6$  K; 4— $6.7$  K; 5— $7.8$  K; 6— $8.8$  K; 7— $13.8$  K.

tional transition shifted to the higher field region and became more spread out, similar to what is observed when measuring magnetization curves. The field interval over which a sharp change in magnetostriction  $\Lambda_c$  along the  $c$  axis occurred, associated with spin reorientation, was appreciably broader than observed for measurements along the  $a$  and  $b$  axes, which is explained by the demagnetization factor of the specimen when measuring  $\Lambda_c$  being three times greater than when measuring  $\Lambda_b$  and  $\Lambda_a$ .

In order to obtain information about the influence of a field  $\mathbf{H} \parallel \mathbf{b}$  on the high-temperature orientational transitions, measurements were made of the thermal expansion for fixed values of the field (Fig. 3). Three kinks were found in the

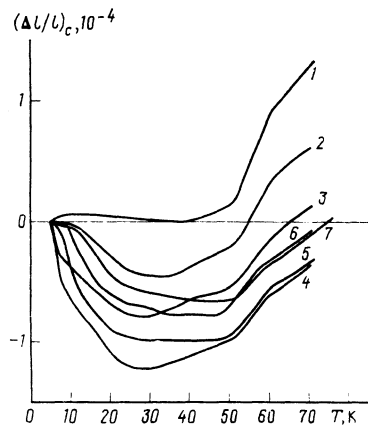


FIG. 3. Thermal expansion of  $\text{HoFeO}_3$  along the  $c$  axis for fixed values of the magnetic field  $\mathbf{H} \parallel \mathbf{b}$ : 1)  $H = 0$  kOe; 2)  $5.04$  kOe; 3)  $25.4$  kOe; 4)  $29.1$  kOe; 5)  $32$  kOe; 6)  $36$  kOe; 7)  $40.5$  kOe.

shape of the thermal expansion curve in the absence of a field at temperatures  $\approx 40, 50, 60$  K, corresponding to three spontaneous orientational phase transitions  $\Gamma_2 \rightarrow \Gamma_{12}$ ,  $\Gamma_{12} \rightarrow \Gamma_{24}$  and  $\Gamma_{24} \rightarrow \Gamma_4$  (Refs. 6 and 7). On applying a field  $\mathbf{H} \parallel \mathbf{b}$  the temperature of the  $\Gamma_2 \rightarrow \Gamma_{12}$  transition (more precisely  $\Gamma_{23} \rightarrow \Gamma_{1234}$ , see below) shifted to lower temperatures with increase in field, while the temperature of the two other transitions changed insignificantly as the field increased.

It was of interest to determine the phases between which orientational transitions took place at low temperatures. Since the initial phase in a magnetic field  $\mathbf{H} \parallel \mathbf{b}$  is  $\Gamma_{23} (G_z F_x F_y)$ , it is evident that the final phase could be either  $\Gamma_{34} (G_x F_z F_y)$  or  $\Gamma_{13} (G_y F_y)$ . Unfortunately in the present case it is a rather complicated problem to determine the final phase from magnetic measurements. As calculation showed, the theoretical magnetization curves in the phases  $\Gamma_{13}$  and  $\Gamma_{34}$  are close to one another and differ appreciably from the magnetization in phase  $\Gamma_{23}$  (the inset in Fig. 1). The change in magnetization  $m_b(H)$  at the orientational transitions  $\Gamma_{23} \rightarrow \Gamma_{34}$  and  $\Gamma_{23} \rightarrow \Gamma_{13}$  should have similar form and differ little from one another, which would make it impossible to determine exactly what type of orientational transition was taking place. The determination of the type of orientational transition is also difficult from a comparison of the magnitudes of magnetostriction observed for different transitions, since the magnetostrictions of the Fe subsystem due to the rotation of the  $\text{Fe}^{3+}$  spins at the  $G_z \rightarrow G_x$  (results for  $\text{YFeO}_3$  and  $\text{HoFeO}_3$  in Refs. 4 and 7 respectively) and  $G_x \rightarrow G_y$  [results for  $\text{Ho}_{0.5}\text{Dy}_{0.5}\text{FeO}_3$ , (Ref. 8)] transitions have the same sign and differ insignificantly in magnitude. It is especially difficult to choose between the transition  $G_z \rightarrow G_x$  and  $G_x \rightarrow G_y$  when considering the magnetostriction

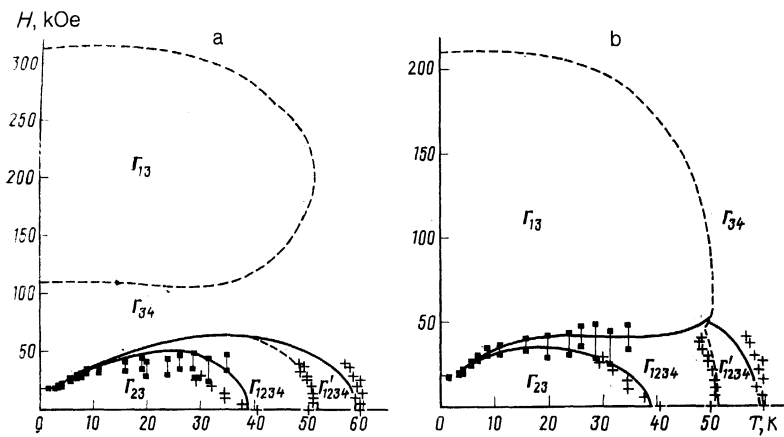


FIG. 4.  $H$ - $T$  phase diagram for  $\text{HoFeO}_3$ , for  $\mathbf{H} \parallel \mathbf{b}$ . The squares and vertical lines are the experimental results for magnetostriction, the crosses are for thermal expansion. The solid lines (second order PT) and the dashed lines (first order PT) are theory. The calculation was carried out for two values of the Ho-Fe isotropic exchange parameter: a)  $a = -140$  kOe; b)  $a = -70$  kOe.

of  $\text{HoFeO}_3$  along the  $b$  axis, since the strong temperature dependence complicates the separation of the contributions to magnetostriction from the R and Fe subsystems.

More information was obtained by measurements of magnetostriction along the  $a$  and  $c$  crystal axes (Fig. 2, a,b), according to which the magnetostriction values obtained by extrapolation to zero field for  $\text{HoFeO}_3$  were  $\Lambda_c = (3.5 \pm 0.4) \cdot 10^{-5}$  and  $\Lambda_a = -(1.2 \pm 0.2) \cdot 10^{-5}$ . Comparison of these values with those obtained for the reorientational transitions  $G_z \rightarrow G_x$  (Ref. 4):  $\Lambda_c = (3.7 \pm 0.4) \cdot 10^{-5}$ , and  $G_z \rightarrow G_y$ :  $\Lambda_c = (4.8 \pm 0.5) \cdot 10^{-5}$  and  $\Lambda_a = -(2.5 \pm 0.3) \cdot 10^{-5}$  makes it possible to choose the transition  $G_z \rightarrow G_x$  ( $\Gamma_{23} \rightarrow \Gamma_{34}$ ) as the most likely transition in  $\text{HoFeO}_3$  for  $\mathbf{H} \parallel \mathbf{b}$ .

The experimental  $H$ - $T$  phase diagram for  $\mathbf{H} \parallel \mathbf{b}$  is shown in Fig. 4. The threshold fields were determined from the kinks of the magnetization and magnetostriction curves. For the high-temperature transitions the phase diagram shows the temperatures corresponding to the kinks in the temperature dependences of  $\Delta l / l$  obtained at fixed values of the field.

### 3. THEORY AND DISCUSSION OF THE RESULTS

In order to describe the observed phase transitions in  $\text{HoFeO}_3$  we will start from the approach developed<sup>6</sup> to harmonize the descriptions of the dynamic and static properties of the system. In this model the Ho subsystem is described in the single-doublet approximation, but taking account of the mixing of the excited states of the  $\text{Ho}^{3+}$  ions, produced by the important Van Vleck contribution to the anisotropy energy of the system. The order parameters of the Ho subsystem are the mean values of the Pauli matrix ( $\sigma = \sigma_x, \sigma_y, \sigma_z$ ) of the  $\text{Ho}^{3+}$  ions in two non-equivalent positions ( $\langle \sigma_{1,2} \rangle$ ) or their linear combination  $\mathbf{f} = (\langle \sigma_1 \rangle + \langle \sigma_2 \rangle) / 2$ ,  $\mathbf{c} = (\langle \sigma_1 \rangle - \langle \sigma_2 \rangle) / 2$ , while the Fe subsystem is characterized as usual by the dimensionless ferro- and antiferromagnetism vectors ( $\mathbf{F}$  and  $\mathbf{G}$ ). The non-equilibrium thermodynamic potentials (TP) are equal to<sup>6</sup> (calculated for 1 molecule of  $\text{HoFeO}_3$ )

$$\Phi(\mathbf{F}, \mathbf{G}, \mathbf{f}, \mathbf{c}) = \Phi_{\text{Fe}}(\mathbf{F}, \mathbf{G}) - \{f_x [(H_x + aF_x)\mu_x + BG_z] + f_z \Delta_{\text{CF}} + c_x \mu_y (H_y + aF_y) + \frac{1}{2} \lambda_f f_x^2 + \frac{1}{2} \lambda_c c_x^2 + \frac{1}{2} T [S(|\langle \sigma_1 \rangle|) + S(|\langle \sigma_2 \rangle|)]\}, \quad (1)$$

where  $\mu_x$  and  $\mu_y$  are the components of the magnetic moment of the quasidoublet of  $\text{Ho}^{3+}$  ions;  $2\Delta_{\text{CF}}$  is its splitting in the crystal field;  $a$  and  $B$  are, respectively, the isotropic

and anisotropic exchange constants of the Ho-Fe interaction;  $\lambda_{f,c}$  are the constants of the Ho-Ho interaction;

$$S(x) = \ln 2 - \frac{1}{2}(1+x) \ln(1+x) - \frac{1}{2}(1-x) \ln(1-x),$$

is the entropy of the two-level system:

$$\begin{aligned} \Phi_{\text{Fe}}(\mathbf{F}, \mathbf{G}) = & \frac{1}{2} A F^2 + \frac{1}{2} D (\mathbf{F}\mathbf{G})^2 - d (F_x G_z - F_z G_x) \\ & - \mu_0 \mathbf{F}\mathbf{H} - \tau_1^{\text{V}} H_x G_z \\ & - \tau_3^{\text{V}} H_z G_x - m_{y0} H_y G_x G_y G_z + \Phi_A^0(\mathbf{G}), \quad (2) \\ \Phi_A^0(\mathbf{G}) = & \frac{1}{2} K_{ac}^0 G_z^2 + \frac{1}{2} K_{ab}^0 G_y^2 + \frac{1}{4} K_2 G_z^4 \\ & + \frac{1}{4} K_2' G_y^4 + \frac{1}{2} K'' G_z^2 G_y^2, \quad (3) \end{aligned}$$

$\Phi_{\text{Fe}}$  is the TP of the Fe subsystem, renormalized by the Van Vleck correction to the energy of the  $\text{Ho}^{3+}$  quasidoublet. The second order renormalization of the anisotropy constants are the most important:

$$K_{ac}^0 = K_{ac}^{\text{Fe}} + K_{ac}^{\text{V}}, \quad K_{ab}^0 = K_{ab}^{\text{Fe}} + K_{ab}^{\text{V}}.$$

On minimizing the TP (Eq. 1) with respect to  $\mathbf{F}$ , taking into account that  $G^2 = 1 - F^2 \approx 1$  and eliminating  $\mathbf{F}$  from Eq. 1, we obtain for  $\Phi$  with  $\mathbf{H} \parallel \mathbf{b}$

$$\begin{aligned} \Phi(\mathbf{G}, \mathbf{f}, \mathbf{c}) = & \Phi_A(\mathbf{G}) - \frac{1}{2} (\chi_{\perp} - \Delta \chi G_y^2) H_y^2 - H_y (m_{y0} G_x G_y G_z \\ & + m_{y1} f_x G_x G_y + m_{y2} c_x G_y^2) - f_x G_z \Delta_{\text{ex}}^0 - f_z \Delta_{\text{CF}} - \mu_y^0 c_x H_y \\ & - \frac{1}{2} f_x^2 (\bar{\lambda}_f - \Delta \lambda_f G_x^2) - \frac{1}{2} c_x^2 (\bar{\lambda}_c - \Delta \lambda_c G_y^2) + \lambda_f f_x c_x G_x G_y \\ & - \frac{1}{2} T [S(|\langle \sigma_1 \rangle|) + S(|\langle \sigma_2 \rangle|)], \quad (4) \end{aligned}$$

where

$$\begin{aligned} \chi_{\perp} = & \mu_0^2 / A \equiv \mu_0 / 2H_E, \quad \Delta \chi \equiv \chi_{\perp} - \chi_{\parallel} = \chi_{\perp} / (1 + A/D), \\ \Delta_{\text{ex}}^0 = & B + \mu_x a d / A, \\ m_{y1} = & -\Delta \chi a \bar{\mu}_x, \quad m_{y2} = -\Delta \chi a \bar{\mu}_y, \quad \mu_y^0 = \mu_y (1 + a / 2H_E), \quad (4a) \\ \bar{\lambda}_{f,c} = & \lambda_{f,c} + \chi_{\perp} (a \bar{\mu}_{x,y})^2, \\ \Delta \lambda_{f,c} = & \Delta \chi (a \bar{\mu}_{x,y})^2, \quad \lambda = (\Delta \lambda_f \Delta \lambda_c)^{1/2}, \quad \bar{\mu}_{x,y} = \mu_{x,y} / \mu_0. \end{aligned}$$

The magnitude of  $\Phi_A(\mathbf{G})$  is determined by Eq. (3), in which we must make the substitution  $K_{ab}^0 \rightarrow K_{ab}^0 + d^2 / A \equiv K_{ab}^{\text{Fe}} + K_{ab}^{\text{V}}$ .

We shall analyze the phase transitions in a magnetic field on the basis of Eq. (4). At low temperatures, when the stable phase is  $\Gamma_2$  ( $G_z F_x$ ), the application of an external field  $\mathbf{H} \parallel \mathbf{b}$  produces a splitting of the quasidoublet levels of  $\text{Ho}^{3+}$ , for certain positions, and an approach for others. In the crossover (approach) region of the lower energy levels of the  $\text{Ho}^{3+}$  ion quasidoublet, the splitting of which for positions 1

and 2 are determined by the expression

$$\Delta_{1,2} = \{[\Delta_{ex}^0 G_x + (\bar{\lambda}_f - \Delta\lambda_f G_x^2) f_{\xi} + (H_y m_{y1} - \lambda c_{\xi}) G_x G_y] \pm [(\mu_y^0 + m_{y2} G_y^2) H_y + (\bar{\lambda}_c - \Delta\lambda_c G_y^2) c_{\xi} - \lambda G_x G_y f_{\xi}]\}^2 + \Delta_{CF}^2, \quad (5)$$

an instability of magnetic structure arises in the system, tending to produce an additional repulsion of the levels.<sup>4,5</sup> This instability must be manifest in the form of the orientational transitions in the Fe subsystem and a sharp magnetic reversal of the  $\text{Ho}^{3+}$  ions in one of the non-equivalent sites, which is the cause of the observed discontinuities on the magnetization curves  $m_b(H)$ . The Fe subsystem should then go over either into the high-temperature phase  $\Gamma_{34}(G_x F_x F_y)$  or into the phase  $\Gamma_{13}(G_y F_y)$ , which is determined by the ratio of the values of the TP for the given external field.

We shall first consider the case  $T = 0$  K, ignoring the splitting  $\Delta_{CF}$ , which in the case of  $\text{HoFeO}_3$  does not play a noticeable part. Minimizing the TP (Eq. 4) with respect to  $\mathbf{G}$ ,  $\mathbf{f}$ , and  $\mathbf{c}$  we obtain the following possible phases:

$$\begin{aligned} A(\Gamma_{23}(G_x F_x F_y)): & G_x=1, f_{\xi}=1, c_{\xi}=0; \\ B(\Gamma_{34}(G_y F_x F_y)): & G_x=1, f_{\xi}=0, c_{\xi}=1; \\ C(\Gamma_{13}(G_y F_y)): & G_y=1, f_{\xi}=0, c_{\xi}=1. \end{aligned} \quad (6)$$

Comparing the values of the TP's for these phases, we obtain for the corresponding fields for transitions between them (first-order phase transitions) the values

$$A \leftrightarrow B: H_{AB} = [\Delta_{ex}^0 - 1/2 K_{ac}^0 - 1/4 K_2 + 1/2 (\bar{\lambda}_f - \bar{\lambda}_c)] / \mu_y^0, \quad (7a)$$

$$\begin{aligned} A \leftrightarrow C: H_{AC} &= H_{AB} + (\Phi_C - \Phi_B) / \mu_y \\ &= H_{AB} + \Delta\chi [(H_{AC} + a\mu_y / \mu_0)^2 - H_{sf}^2] / \mu_y, \end{aligned} \quad (7b)$$

$$C \leftrightarrow B: H_{CB}^{\pm} = -a\mu_y / \mu_0 \pm H_{sf}, \quad (7c)$$

where  $\Phi_C$  and  $\Phi_B$  are the TP of the phases  $C$  and  $B$  respectively, and

$$H_{sf} = [-1/2 K_{ab}^0 + 1/4 K_2] / \Delta\chi^{1/2} \quad (8)$$

is a quantity with the meaning of the field of a spin-flop transition  $G_y \rightarrow G_x$  ( $\Gamma_1 \rightarrow \Gamma_4$ ) in the Fe subsystem. The fields for the transitions  $A \leftrightarrow B$  and  $B \leftrightarrow C$  due to instability produced by level crossing are extremely close to one another and are mainly determined for  $\text{HoFeO}_3$  by the value  $H_0 = \Delta_{ex} / \mu_y \approx 10$  kOe. Into which of the possible phases ( $B$  or  $C$ ) the system will land is determined by the difference between the energies of these phases, or in the present case by the ratio of the values of  $H_{sf}$  and  $H_{AC} + a\mu_y / \mu_0 \approx a\mu_y / \mu_0$ . An estimate of  $H_{sf}$  for  $\text{HoFeO}_3$ , using results of Balbashov *et al.*,<sup>6</sup> gives the value  $\sim 10^5$  Oe; of the same order is the quantity  $a\mu_y / \mu_0$  [ $a \sim -10^5$  Oe according to the results for  $\text{DyFeO}_3$  (Ref. 9) and  $\text{GdFeO}_3$  (Ref. 10)].

The character of the phase transitions in  $\text{HoFeO}_3$  will thus depend strongly on the magnitude of the isotropic exchange constant. Unfortunately this quantity has not been determined in  $\text{HoFeO}_3$ . Therefore, in order to encompass all possible situations, we studied the dependence of the transition fields [Eq. (7)] on  $a$  and constructed the corresponding phase diagram (Fig. 5), illustrating the sequence of phase transitions in  $\text{HoFeO}_3$  at  $T = 0$  K as a function of  $a$ . It can be seen that for  $a$  in the range  $a^- < a < a^+$ , where  $a^{\pm} \approx (\pm H_{sf} - H_0) \mu_0 / \mu_y$ , the instability associated with level crossing appears as a SR transition to phase  $C$  ( $\Gamma_{13}$ ),

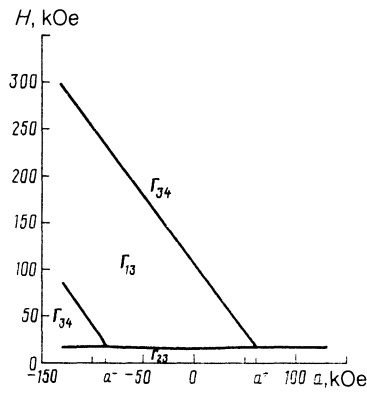


FIG. 5.  $H$ - $a$  phase diagram at  $\mathbf{H} \parallel \mathbf{b}$  for  $\text{HoFeO}_3$  and  $T = 0$  K.

while outside this interval as a SR transition to phase  $B$  ( $\Gamma_{34}$ ).

If, however, for large positive  $a$  ( $a > a^+$ ) nothing takes place in the system with further increase in field, then for large negative  $a$  ( $a < a^-$ ) another two SR transitions are possible:  $B \rightarrow C$  ( $\Gamma_{34} \rightarrow \Gamma_{13}$ ) and  $C \rightarrow B$  ( $\Gamma_{13} \rightarrow \Gamma_{34}$ ). Whereas the latter has the meaning of an ordinary spin-flop transition, then the former is an inverse spin-flop transition, i.e., a transition from a weak ferromagnetic phase ( $\Gamma_{34}$ ) in which the vector  $\mathbf{G}$  is perpendicular to the external field, to an antiferromagnetic phase ( $\Gamma_{13}$ ) in which the vector  $\mathbf{G}$  lies along the field. The physical reason for the inverse spin-flop transition is that the external field  $H_y$  and the field  $ac_{\xi}\mu_y / \mu_0$  ( $c \sim 1$  in large fields), associated with the isotropic Ho-Fe exchange and acting on the Fe sublattice, are directed oppositely to one another for  $a < 0$ . Therefore, at first the modulus of the total field  $H_{\text{eff}} = H_y + ac_{\xi}\mu_y / \mu_0$  will decrease, remaining negative. As a result, the energy gain associated with canting (sloping) of the magnetic moments of the Fe sublattice ( $\frac{1}{2}\chi_1 H_{\text{eff}}^2$ ) will for a certain  $H_y$  become less than the anisotropy energy, stabilizing the  $\Gamma_{13}(G_y)$  phase to which the system will go over. Further increase in the field, depending on the extent to which it is compensated in  $H_{\text{eff}}$  by the negative exchange contribution, leads finally to the usual spin-flop transition.

At high temperatures when  $c_{\xi} = \mu_y H_y / T \ll 1$ , the picture considered changes and the behavior of the system becomes similar to an ordinary antiferromagnet in which an the external field amplified by  $1 + \eta_y$  times acts, since  $H_{\text{eff}} = H_y (1 + \eta_y)$ , where  $\eta_y = a\mu_y^2 / \mu_0 T$  (Ref. 4).

We shall now consider the phase transitions for finite temperatures and analyze the  $H$ - $T$  phase diagram of  $\text{HoFeO}_3$  for  $\mathbf{H} \parallel \mathbf{b}$ . As analysis of the TP shows (Eq. 4),<sup>4</sup> the possible phases in the system are  $A(\Gamma_{23})$ ,  $B(\Gamma_{34})$ ,  $C(\Gamma_{13})$  and the angular spatial phase  $D(\Gamma_{1234})$ . We will give the values of the order parameters  $\mathbf{G}$ ,  $\mathbf{F}$ ,  $\mathbf{c}$  in these phases and the regions of their stability.

$$\begin{aligned} \text{Phase } A(\Gamma_{23}(G_x F_x F_y)): & |G_x| = 1, \\ f_{\xi} &= [\Delta_{ex}^0 (\kappa^+ - \bar{\lambda}_c \eta) + h\kappa^-] / d, \quad c_{\xi} = f_{\xi} = \Delta_{CF} \kappa^-, \\ c_{\xi} &= [h(\kappa^+ - \bar{\lambda}_f \eta) + \Delta_{ex}^0 \kappa^-] / d. \end{aligned} \quad (9)$$

where

$$\begin{aligned} d &= 1 - \kappa^+ (\bar{\lambda}_f + \bar{\lambda}_c) + \bar{\lambda}_f \bar{\lambda}_c \eta, \quad \kappa^{\pm} = (\sigma_1 / \Delta_1 \pm \sigma_2 / \Delta_2) / 2, \\ \eta &= \sigma_1 \sigma_2 / \Delta_1 \Delta_2, \quad h = \mu_y^0 H_y, \quad \sigma_{1,2} = \text{th}(\Delta_{1,2} / T), \end{aligned}$$

while the half-splittings  $\Delta_{1,2}$  of the  $\text{Ho}^{3+}$  ion quasidoublet, corresponding to its two non-equivalent positions 1 and 2, are determined by the equations

$$\Delta_{1,2}^2 = [\Delta_{ex}^0 (1 - \tilde{\lambda}_c (\kappa^+ \mp \kappa^-)) \pm h (1 - \tilde{\lambda}_f (\kappa^+ \mp \kappa^-))]^2 / d^2 + \Delta_{CF}^2 \quad (10)$$

The stability regions of this phase and of other phases are found by standard means from the condition of positive-definiteness of the quadratic form made up of the second derivatives of the TP with respect to the order parameters  $\theta, \varphi, \mathbf{f}, \mathbf{c}$ , where  $\varphi$  and  $\theta$  are given by the orientation of the vector  $\mathbf{G}$ . As a result, we obtain for the stability region of the phase  $\Gamma_2$

$$\tilde{K}_{ca} \tilde{K}_{cb} - [m_{y0} H_y - f_\xi \Delta \chi a \tilde{\mu}_x (H_y + a c_\xi \tilde{\mu}_y)]^2 \geq 0, \quad \tilde{K}_{ca}, \tilde{K}_{cb} \geq 0, \quad (11)$$

where

$$\tilde{K}_{ca} = K_{ca}^0 + \Delta_{ex}^0 f_\xi + \Delta \chi (a f_\xi \tilde{\mu}_x)^2, \quad K_{ca}^0 = -K_{ac}^0 - K_2, \quad (12)$$

$$\tilde{K}_{cb} = K_{cb}^0 + \Delta_{ex}^0 f_\xi + \Delta \chi (H_y + a c_\xi \tilde{\mu}_y)^2, \quad K_{cb}^0 = K_{ab}^0 + K_2'' + K_{ca}^0.$$

Here  $\tilde{K}_{ca}, \tilde{K}_{cb}$  (and the analogous quantities below) have the meaning of effective magnetic-field-dependent anisotropy constants in the corresponding crystals planes, which go over into the usual anisotropy constants for  $H \rightarrow O$ .

Phase B ( $\Gamma_{34} (G_x F_z F_y)$ ):  $|G_x| = 1$ ,

$$f_\xi = 0, \quad f_\zeta = (\Delta_{CF}/\Delta) \sigma, \quad c_\xi = c_\xi^0 = h\sigma / (\Delta - \tilde{\lambda}_c \sigma), \quad c_\zeta = (\Delta_{CF}/\Delta) \sigma, \quad (13)$$

where  $\sigma = \tanh (\Delta/T)$ , with the semi-splitting  $\Delta$  found from the equation

$$\Delta^2 = h^2 / (1 - \tilde{\lambda}_c \sigma / \Delta)^2 + \Delta_{CF}^2. \quad (14)$$

Stability is determined by the inequalities

$$\tilde{K}_{ac} \tilde{K}_{ab} - H_y^2 (m_{y0} + m_y')^2 \geq 0, \quad \tilde{K}_{ac}, \tilde{K}_{ab} \geq 0, \quad (15)$$

where

$$\tilde{K}_{ac} = K_{ac}^0 - (\Delta_{ex}^0)^2 / (T - \lambda_f'),$$

$$\tilde{K}_{ab} = K_{ab}^0 + \Delta \chi H_y^2 (1 + \eta_y)^2 (1 - \varepsilon_1),$$

$$m_y' = -\Delta_{ex}^0 \Delta \chi \tilde{\mu}_x a (1 + \eta_y) / (T - \lambda_f'), \quad \lambda_f' = \tilde{\lambda}_f - \Delta \lambda_f,$$

$$\eta_y = \tilde{\mu}_y \mu_y^0 a \sigma / (\Delta - \tilde{\lambda}_c \sigma), \quad \varepsilon_1 = \Delta \chi a^2 \tilde{\mu}_y^2 / (T - \lambda_f'), \quad (16)$$

$$\tilde{T} = T / [(1 - \sigma^2) \sin^2 \gamma + (\sigma T / \Delta) \cos^2 \gamma], \quad \text{tg } \gamma = h / \Delta_{CF} (1 - \tilde{\lambda}_c \sigma / \Delta).$$

Phase C ( $\Gamma_{13} (G_y F_y)$ ):  $|G_y| = 1$ ,

$$f_\xi = 0, \quad f_\zeta = (\Delta_{CF}/\Delta) \sigma, \quad c_\xi = c_\xi^0, \quad c_\zeta = (\Delta_{CF}/\Delta) \sigma.$$

The stability condition is

$$\tilde{K}_{bc} \tilde{K}_{ba} - H_y^2 (m_{y0} + m_y')^2 \geq 0, \quad \tilde{K}_{bc}, \tilde{K}_{ba} \geq 0, \quad (17)$$

where

$$\tilde{K}_{ba} = K_{ba}^0 - \Delta \chi H_y^2 (1 + \eta_y)^2 (1 + \varepsilon_1), \quad K_{ba}^0 = -K_{ab}^0 - K_2',$$

$$\tilde{K}_{bc} = K_{bc}^0 - (\Delta_{ex}^0)^2 / (T - \tilde{\lambda}_f) - \Delta \chi H_y^2 (1 + \eta_y)^2,$$

$$K_{bc}^0 = K_{ac}^0 + K_2'' + K_{ba}^0.$$

The values of  $c^0, \Delta, m_y', \eta_y, \varepsilon_1, \tilde{T}$  are determined from the same formulae as in phase B, but with the substitution

$$\tilde{\lambda}_c \rightarrow \lambda_c' = \tilde{\lambda}_c - \Delta \lambda_c, \quad \lambda_f' \rightarrow \tilde{\lambda}_f,$$

$$\mu_y^0 \rightarrow \mu_y' = \mu_y^0 + m_{y2} = \mu_y [1 + (\chi_{\perp} - \Delta \chi) a / \mu_0] \approx \mu_y.$$

Phase D ( $\Gamma_{1234} (G_x G_y G_z F_x F_y F_z)$ ):

$$G_x = \sin \theta_0 \cos \varphi_0, \quad G_y = \sin \theta_0 \sin \varphi_0, \quad G_z = \cos \theta_0,$$

$$f_\xi, f_\zeta \neq 0, \quad c_\xi, c_\zeta \neq 0.$$

The equations for  $\theta, \varphi, \mathbf{f}, \mathbf{c}$  in this phase and the conditions for its stability are extremely involved. We will therefore not give them but limit ourselves to a qualitative picture which is confirmed by numerical calculations (see below). There are here two types of stable state (solution) corresponding to the spatial orientations of  $\mathbf{G}$ : close to the  $ac$  plane ( $\varphi_{01} \approx 0$ , phase  $D_1$ ) and close to the  $bc$  plane ( $\varphi_{02} \approx \pi/2$ , phase  $D_2$ ). The appearance of spatially equilibrium states is due to terms of the form  $m_{y0} G_x G_y G_z H_y$  (Ref. 11) and  $m_{y1} f_x G_x G_y H_y$  in the TP,<sup>4</sup> thanks to which the vector  $\mathbf{G}$  is inclined to the  $ac$  plane if the initial angular phase was  $\Gamma_{24}$ , or to the  $bc$  plane if it was the  $\Gamma_{12}$  phase. Thus the instability of any collinear phase [ $\Gamma_4 (G_x), \Gamma_1 (G_y), \Gamma_2 (G_z)$ ] leads to reorientation of  $\mathbf{G}$  not into the plane of the angular phase of the type  $G_x G_z$  or  $G_y G_z$ , but immediately into the spatial phase  $G_x G_y G_z$ , in which the vector  $\mathbf{G}$  lies either close to the  $ac$  plane in one case, or to the  $bc$  plane in the other. An isostructural spin reorientation PT is possible between the angular spatial phases  $D_1$  and  $D_2$  indicated, i.e. a transition at which the magnetic symmetry of the phases does not change. The observed line on the  $H$ - $T$  phase diagram in the region  $T \approx 50$  K (Fig. 4) corresponds to just such a PT.

To determine the fields of the phase transitions and to construct the  $H$ - $T$  phase diagram for  $\text{HoFeO}_3$  with  $\mathbf{H} \parallel \mathbf{b}$  we will use the parameters of the magnetic interaction system which enter into the TP [Eqs. (1) and (4)], which were found in Eq. (6):  $\Delta_{ex}^0 = 4.7$  K,  $\Delta_{CF} = 2.4$  K,  $\lambda_f = -3.5$  K,  $\lambda_c = -2.5$  K,  $\mu_y = 7.2 \mu_B$ ,  $H_E = 8 \cdot 10^6$  Oe,  $K_2 = 0.07$  K,  $K_2' = -0.12$  K, and  $K_2'' = -0.07$  K. We will write the anisotropy constants  $K_{ac}^0(T)$  and  $K_{ab}^0(T)$ , taking account of the temperature dependence of the Van Vleck contribution, in the form

$$K_{ac,ab}^0(T) = K_{ac,ab}^{Fe} + K_{ac,ab}^{VV} = K_{ac,ab}^0 + [e_2 K_{ac,ab}^{(2)} + e_3 K_{ac,ab}^{(3)}] / Z_0,$$

where  $Z_0 = 1 + e_2 + e_3$ ;  $e_i = \exp(-E_i/T)$ ;  $E_i$  is the energy of the excited states (quasidoublets) of the  $\text{Ho}^{3+}$  ion in the crystal field ( $E_2 = 120$  K,  $E_3 = 250$  K),  $K_{ac,ab}^0 = K_{ac,ab}^{Fe} + K_{ac,ab}^{(1)}$ ; the magnitudes of  $K_{ac,ab}^{(1)}$  characterize the anisotropy in the shift of energy levels of the  $\text{Ho}^{3+}$  ion for reorientation of  $\mathbf{G}$  from the  $a$  axis to the  $b$  or  $c$  crystal axis. According to Balbashov *et al.*  $K_{ac}^{(1)} = 0.3$  K,  $K_{ac}^{(2)} = 0.72$  K,  $K_{ac}^{(3)} = -0.6$  K,  $K_{ab}^{(1)} = -0.173$  K,  $K_{ab}^{(2)} = 2.7$  K, and  $K_{ab}^{(3)} = 1.2$  K. Since the value of the isotropic exchange constant  $a$  is not known for  $\text{HoFeO}_3$ , we have, guided by the results of Zvezdin and Matveev<sup>9</sup> for  $\text{DyFeO}_3$  and of Belov *et al.*<sup>10</sup> for  $\text{GdFeO}_3$ , according to which  $a \sim -10^5$  Oe, chosen it by starting from the best agreement between the experimental and theoretical  $H$ - $T$  phase diagrams.

Calculations showed the high sensitivity of the shape of the  $H$ - $T$  phase diagram to the magnitude of the constant  $a$ . This follows directly from the  $H$ - $a$  phase diagram (Fig. 5), according to which at  $T = 0$  K for  $a > a^- \approx -87$  kOe the PT should be accomplished according to the scheme  $\Gamma_{23} \rightarrow \Gamma_{13} \rightarrow \Gamma_{34}$ , while for  $a < a^-$  according to the scheme  $\Gamma_{23} \rightarrow \Gamma_{34} \rightarrow \Gamma_{13} \rightarrow \Gamma_{34}$ , while the fields for the PT's  $\Gamma_{23} \rightarrow \Gamma_{13}$  and  $\Gamma_{23} \rightarrow \Gamma_{34}$  practically coincide with one another.<sup>2)</sup>

Figure 4 shows the  $H$ - $T$  phase diagrams for the two variants of the phase transitions indicated, calculated for  $a = -140$  kOe (Fig. 4,a) and  $a = -70$  kOe (Fig. 4,b). The lines of the second-order PTs  $\Gamma_{23} \rightarrow \Gamma_{1234}$ ,  $\Gamma_{34} \rightarrow \Gamma_{1234}$  and  $\Gamma_{13} \rightarrow \Gamma_{1234}$  are calculated from the conditions of Eqs. (11), (15), and (17), while the lines of the first order PTs  $\Gamma_{23} \rightarrow \Gamma_{34}$ ,  $\Gamma_{13} \rightarrow \Gamma_{34}$  and  $\Gamma_{13} \rightarrow \Gamma'_{1234}$  from the condition of the equality of the TP's of the corresponding phases. It is seen from Fig. 4 that in the cases  $a$  and  $b$  the lower parts of the phase diagram ( $H < 50$  kOe) essentially agree with one another, while the upper parts differ qualitatively. Thus, in the first case (a) the following sequence of phase transitions is realized in the system as the field increases at low temperatures:  $\Gamma_{23} \rightarrow \Gamma_{34} \rightarrow \Gamma_{13} \rightarrow \Gamma_{34}$  ( $A \rightarrow B \rightarrow C \rightarrow D$ ), i.e., instability arises at first, due to the approach of the lower levels of the  $\text{Ho}^{3+}$  ions as, manifest by their sharp magnetic reversal (Fig. 1) and reorientation of  $\mathbf{G}$  from the  $c$  to the  $a$  axis ( $G_z \rightarrow G_x$ ) at  $H_y \approx 20$  kOe, while for  $H_y \approx 110$  kOe an inverse spin-flop transition takes place ( $G_y \rightarrow G_x$ ) and, finally, for very high fields ( $\approx 250$  kOe) the usual spin-flop transition ( $G_x \rightarrow G_y$ ) is realized. In the second case (b) the sequence of transitions is different:  $\Gamma_{23} \rightarrow \Gamma_{13} \rightarrow \Gamma_{34}$  ( $A \rightarrow C \rightarrow B$ ), i.e., the instability arising on the approach of the lower energy levels of the  $\text{Ho}^{3+}$  ions with increasing field, leads to a reversal of  $\mathbf{G}$ , from the  $c$  to the  $b$  axis ( $G_z \rightarrow G_y$ ), while in large fields, as in the preceding case, a spin-flop transition occurs ( $G_y \rightarrow G_x$ ).

Our experimental investigation of magnetostriction in magnetic fields up to 60 kOe show (see Sec. 2) that the PT for  $\mathbf{H} \parallel \mathbf{b}$ ,  $H \approx 20$  kOe apparently goes from phase  $\Gamma_{23}$  to phase  $\Gamma_{34}$ . This permits a choice to be made in favor of the phase diagram shown in Fig. 4a. The choice of the value  $a = -140$  kOe for this phase diagram was determined from the fact that for a value of  $a$  smaller in absolute magnitude there should be observed in fields of 60 kOe not one PT, as occurred in our experiment, but two PTs:  $\Gamma_{23} \rightarrow \Gamma_{34}$ ,  $\Gamma_{34} \rightarrow \Gamma_{13}$  (Fig. 5).

Taking account of the richness of the phase diagram of  $\text{HoFeO}_3$  and the possibility of observing unusual phase transitions such as an inverse spin-flop transition, which is possible at  $a < 0$ , a further experimental study of  $\text{HoFeO}_3$  in strong fields would be of undoubted interest, using methods which would allow a direct determination of the magnetic structure (neutron diffraction, Mössbauer effect), since magnetostriction, after all, provides indirect information on the type of magnetic structure.

#### 4. CONCLUSIONS

The investigations of the magnetic and magnetostriction properties of  $\text{HoFeO}_3$  in a magnetic field  $\mathbf{H} \parallel \mathbf{b}$  and the corresponding theoretical analysis made it possible to determine the nature of the phase transitions in a field and to construct experimental (for  $H < 60$  kOe) and theoretical  $H$ - $T$  phase diagrams for  $\text{HoFeO}_3$ , which agree between themselves on the whole. The important features of the phase diagrams of  $\text{HoFeO}_3$  are: a) the existence of instability which arises on the approach of the lower energy levels of the  $\text{Ho}^{3+}$  ions and is manifest in the sharp magnetic reversal at low temperatures with a simultaneous reorientation of the spins of the Fe subsystem; b) the existence of two spatial angular phases ( $\Gamma_{1234}$  and  $\Gamma'_{1234}$ ) and an isostructural SR

first order transition between them; c) the possible existence (for  $a < a^-$ ) in the region of fairly high fields ( $H \geq 100$  kOe) of an unusual SR transition, at which the spins of the  $\text{Fe}^{3+}$  ions reorient from a state perpendicular to a state parallel to the external field ( $\Gamma_{34} \rightarrow \Gamma_{13}$ ) (an inverse spin-flop transition). As is shown in this work, the mechanism of this transition is determined by the action on the spins of the  $\text{Fe}^{3+}$  ions not only by the external field, but also by the internal exchange field due to the negative R-Fe isotropic exchange ( $a < 0$ ), which is directed oppositely to the external. The total effective field does not therefore increase at first, but decreases with increasing external field, which leads to the inverse spin-flop transition, and with further increase in external field  $\mathbf{H} \parallel \mathbf{b}$  to the usual spin-flop transition. The strong dependence of the topology of the high-field part of the  $H$ - $T$  phase diagram of  $\text{HoFeO}_3$  for  $\mathbf{H} \parallel \mathbf{b}$  on the magnitude and sign of the constant  $a$  of the isotropic R-Fe exchange, which in orthoferrites does not usually play a noticeable role, is associated with the appearance of such a competition of the external magnetic field and the internal exchange field. In the case of  $\text{HoFeO}_3$  the role of R-Fe exchange is manifest thanks to the large Van Vleck contribution to the anisotropy energy of the crystal, stabilizing the antiferromagnetic phase  $\Gamma_1$  ( $G_y$ ) and leading finally, on balancing of the internal and external fields, to an inverse spin-flop transition into the state  $\mathbf{H} \parallel \mathbf{G} \parallel \mathbf{b}$ .

We note that similar inverse spin-flop transitions in a field  $\mathbf{H} \parallel \mathbf{b}$  are also possible in other orthoferrites (orthochromates) having a tendency to a spontaneous SR transition into the antiferromagnetic state  $\Gamma_1$  ( $G_y$ ), for example in  $\text{DyFeO}_3$  (Ref. 10).

<sup>1)</sup> In the numerical calculations we have neglected the small quantity  $m_{y0} = 0$  and only considered the invariant  $m_{y1} f_x G_x G_y H_y$ , for which the magnitude of  $m_{y1}$  is evaluated from the known parameters of the system [see Eq. (4a)].

<sup>2)</sup> It should be noted that for positive values  $a \gg a^+ \approx 60$  kOe an orientational transition  $\Gamma_{23} \rightarrow \Gamma_{34}$  should also be observed, but as calculation showed, it is then not possible to reach agreement between the experimental and theoretical phase diagrams in the temperature interval 40–50 K; we have therefore limited ourselves to an analysis of the phase diagrams for negative values of  $a$ .

<sup>1)</sup> Y. Allain, J. E. Bouree, J. Denis, J. Phys. (Paris) Suppl. C 1, 494 (1971).

<sup>2)</sup> H. Schuchert, S. Hüfner, and R. Faulhaber, Z. Phys. 220, 280 (1969).

<sup>3)</sup> J. C. Walling and R. L. White, Phys. Rev. 10, 4748 (1974).

<sup>4)</sup> K. P. Belov, A. K. Zvezdin, and A. M. Kadomtseva and R. Z. Levitin, *Orientalional Transitions in Rare-Earth Magnets* [in Russian], Nauka, Moscow, 1979.

<sup>5)</sup> A. K. Zvezdin, V. M. Matveev, A. A. Mukhin, and A. I. Popov, *Rare-Earth Ions in Magnetically Ordered Crystals* [in Russian], Nauka, Moscow, 1985.

<sup>6)</sup> A. K. Balbashov, G. V. Kozlov, S. P. Lebedev, A. A. Mukhin, A. Yu. Pronin, and A. S. Prokhorov, Zh. Eksp. Teor. Fiz. 95, 1092 (1989) [Sov. Phys. JETP 68, 629 (1989)]; *Kratk. Soobshch. Fiz.* No 9, 21 (1988); Preprint, IOF AN SSSR No 97, 1988.

<sup>7)</sup> G. P. Vorob'ev, A. M. Kadomtseva, I. B. Krynetskiĭ, and A. A. Mukhin, Zh. Eksp. Teor. Fiz. 95, 1049 (1989) [Sov. Phys. JETP 68, 604 (1989)]. Proc. 23rd all-Union Conf. on Physics of Magnetic Phenomena, Kalinin, Part 3, 708 (1988).

<sup>8)</sup> I. B. Krynetskiĭ, Thesis, Moscow State University, 1974.

<sup>9)</sup> A. K. Zvezdin and V. M. Matveev, Zh. Eksp. Teor. Fiz. 77, 1076 (1979) [Sov. Phys. JETP 50, 543 (1979)].

<sup>10)</sup> D. V. Belov, A. K. Zvezdin, A. M. Kadomtseva, I. B. Krynetskiĭ, A. S. Moskvina, and A. A. Mukhin, Fiz. Tverd. Tela (Leningrad) 23, 2831 (1981) [Sov. Phys. Solid State 23, 1654 (1981)].

<sup>11)</sup> A. P. Agafonov and A. S. Moskvina, Fiz. Tverd. Tela (Leningrad) 30, 612 (1988) [Sov. Phys. Solid State 30, 353 (1988)].

Translated by Robert Berman